Transition Metal Polysulfide Complexes as Single-Source Precursors for Metal Sulfide Nanocrystals

ARTICLE *in* THE JOURNAL OF PHYSICAL CHEMISTRY C · FEBRUARY 2010

Impact Factor: 4.77 · DOI: 10.1021/jp910354q

3 AUTHORS, INCLUDING:

Richard D Tilley
University of New South Wales
98 PUBLICATIONS **2,546** CITATIONS

Transition Metal Polysulfide Complexes as Single-Source Precursors for Metal Sulfide Nanocrystals

John H. L. Beal,*,†,‡,§ Pablo G. Etchegoin,†,‡ and Richard D. Tilley†,‡

School of Chemical and Physical Sciences and The MacDiarmid Institute for Advanced Materials and Nanotechnology, Victoria University of Wellington, P.O. Box 600, Wellington 6140, New Zealand

Received: October 29, 2009; Revised Manuscript Received: January 20, 2010

The metal polysulfide complexes $[M(N\text{-MeIm})_6]S_8$ (M = Fe, Ni) and $ZnS_6(N\text{-MeIm})_2$ (N-MeIm = N-methylimidazole) were synthesized and used as single-source precursors for the synthesis of metal sulfide nanocrystals. Rapid injection of $[Ni(N\text{-MeIm})_6]S_8$ into oleylamine at 300 °C, followed by immediate cooling, led to the formation of spherical, monodisperse 6 nm NiS_2 nanocrystals. Whereas reaction of $[Ni(N\text{-MeIm})_6]S_8$ by gradual heating in oleylamine to 300 °C led to the formation of irregularly shaped 45 nm α-$Ni_{1-x}S$ nanocrystals. Rapid injection of $[Fe(N\text{-MeIm})_6]S_8$ into oleylamine at 300 °C, followed by immediate cooling, led to the formation of 16 nm Fe_3S_4 nanocrystals. Whereas reaction of $[Fe(N\text{-MeIm})_6]S_8$ in oleylamine at 300 °C for 4 h led to the formation of faceted, submicrometer $Fe_{1-x}S$ crystallites. Reaction of $ZnS_6(N\text{-MeIm})_2$ in oleylamine at 300 °C for 30 min led to the formation of monodisperse 11 × 5 nm ZnS nanorods. Metal polysulfide complexes were shown to be viable single-source precursors for a range of transition metal sulfide nanocrystals, with all samples demonstrating a high degree of crystallinity and excellent phase-purity.

Introduction

In recent years much attention has been given to the synthesis and characterization of nanocrystals due to the alterations in the optical,[1] magnetic[2] and catalytic properties[3] which occur in nanometer-sized particles. The transition metal sulfides have featured prominently among the phases investigated in nanocrystalline form - especially nanocrystals of CdS[4,5] and the wide-band gap semiconductor ZnS.[6−8] Other transition metal sulfide nanocrystals to have been investigated include members of the magnetic iron sulfide[9] and nickel sulfide[10,11] phase systems, as well as MnS,[5] Ag_2S,[5] and several copper sulfide phases.[5,12]

Single-source precursors, where the source of the metal and nonmetal component of the target binary compound are contained within a single precursor species, have come to be used widely in nanocrystal synthesis.[13−15] Single-source precursors typically offer the benefit of ease of use, and produce high quality products under relatively mild reaction conditions.[14,15] Single-source precursors have been used previously for the synthesis of transition metal sulfide nanocrystals including ZnS,[14,16,17] iron sulfide,[18,19] and nickel sulfide[20,21] nanocrystals. All of these single-source precursors took the form of metal complexes which included sulfur-containing organic ligands, such as alkyldithiocarbamates,[16,18] thiolates,[19] thiocarboxylates,[14,21] or mercaptobenzothiazole.[20]

In contrast to the metalorganic coordination complexes mentioned above, which have been widely investigated, metal complexes which contain sulfur in the form of inorganic polysulfide ligands appear not to have been investigated previously as single-source precursors for nanocrystals. Metal polysulfide complexes appeared to us to be promising candidates for use as single-source precursors, as they can be easily and simply prepared from cheap starting materials. In addition, decomposition of metal polysulfide complexes to binary metal sulfides was predicted to be facile because, in contrast to metalorganic single-source precursors, no decomposition of organic moieties to liberate sulfur would be required.

Rauchfuss and co-workers first demonstrated that metal polysulfide complexes could be synthesized from metal powder and elemental sulfur with the use of a suitable stabilizing amine ligand.[22−27] The substituted aromatic amine N-methylimidazole (N-MeIm) was found by Rauchfuss and co-workers to be a particularly effective stabilizing ligand and enabled the formation of polysulfide complexes with a variety of metals ([Mg, Mn, Fe, and Ni],[24] Cu,[22] and Zn[23]). It was therefore decided to investigate three such complexes, $[M(N\text{-MeIm})_6]S_8$ (M = Fe, Ni) and $ZnS_6(N\text{-MeIm})_2$, for use as single-source precursors for metal sulfide nanocrystals.

Experimental Methods

Oleylamine (OAm, tech. ≥ 70%) was purchased from Fluka and was distilled under reduced pressure (bp 148 − 176 °C at 0.3 mmHg, colorless liquid) and then stored under nitrogen. $[M(N\text{-MeIm})_6]S_8$ (M = Fe, Ni) and $ZnS_6(N\text{-MeIm})_2$ were synthesized following the procedures of Rauchfuss and co-workers[23,24] (see the Supporting Information for details of syntheses). The metal polysulfide complexes were stored under nitrogen, but could be transferred in air without use of special precautions. Nanocrystal syntheses were performed using standard inert atmosphere techniques.

Synthesis of NiS_2 Nanocrystals. $[Ni(N\text{-MeIm})_6]S_8$ (0.284 g, 3.5×10^{-4} mol, crimson powder) was dissolved in OAm (11 cm^3) to give a crimson solution. This solution was injected rapidly into OAm (40 cm^3) preheated to 300 °C. The reaction mixture became black immediately after injection. The reaction mixture was cooled rapidly, diluted with acetone (50 cm^3) and centrifuged to produce a black precipitate and clear yellow

* To whom correspondence should be addressed. E-mail: j.beal@trinitybioactives.com.

† School of Chemical and Physical Sciences, Victoria University of Wellington.

‡ The MacDiarmid Institute of Advanced Materials and Nanotechnology.

§ Current address: Trinity Bioactives Ltd., P.O. Box 15135, Wellington 6243, New Zealand.

10.1021/jp910354q
Published on Web 02/17/2010

supernatant. The supernatant was discarded and the precipitate was resuspended in toluene (20 cm^3). Acetone (50 cm^3) was added and the suspension was centrifuged to give a black precipitate and a clear, colorless supernatant. This procedure was repeated twice and the precipitate was dried overnight in vacuo.

Synthesis of α-$Ni_{1-x}S$ Nanocrystals. $[Ni(N\text{-MeIm})_6]S_8$ (0.275 g, 3.4×10^{-4} mol, crimson powder) was dissolved in OAm (50 cm^3) to give a crimson solution. This solution was heated to 300 °C. When this temperature was reached, the reaction mixture flocculated to produce black flocks and a clear, yellow supernatant. The reaction mixture was allowed to cool, and centrifuged to give a black precipitate and a clear yellow supernatant. The supernatant was discarded and the precipitate was resuspended in toluene (20 cm^3), then centrifuged to give the precipitate and a clear, colorless supernatant. The supernatant was discarded and this procedure was repeated, this time with the addition of acetone (80 cm^3) to destabilize the toluene suspension. The precipitate was dried in vacuo overnight, then ground into a dark black powder.

Synthesis of Fe_3S_4 Nanocrystals. $[Fe(N\text{-MeIm})_6]S_8$ (0.711 g, 8.8×10^{-4} mol, purple crystals) was dissolved in OAm (10 cm^3) to give a black solution. This solution was rapidly injected into a flask containing OAm (40 cm^3) preheated to 300 °C. The black reaction mixture was rapidly cooled immediately after injection by lifting the flask out of the heating mantle, and centrifuged to give a black precipitate and a clear yellow supernatant. The supernatant was discarded, and the precipitate was suspended in toluene (20 cm^3), then centrifuged to give the precipitate and a clear, colorless supernatant. The supernatant was discarded and this procedure was repeated, this time with the addition of acetone (80 cm^3) to destabilize the toluene suspension. The precipitate was dried in vacuo overnight, then ground into a dark black powder.

Synthesis of $Fe_{1-x}S$ Nanocrystals. $[Fe(N\text{-MeIm})_6]S_8$ (0.406 g, 5.0×10^{-4} mol, purple crystals) was dissolved in OAm (50 cm^3) to give a black solution. The solution was heated to 300 °C and held at this temperature for 4 h, then allowed to cool. The black reaction mixture was centrifuged to give a black precipitate and a clear yellow supernatant. The supernatant was discarded and the precipitate was suspended in toluene (20 cm^3), then centrifuged to give the precipitate and a clear, colorless supernatant. The supernatant was discarded and this procedure was repeated, this time with the addition of acetone (80 cm^3) to destabilize the toluene suspension. The precipitate was dried in vacuo overnight, then ground into a dark black powder.

Synthesis of ZnS Nanorods. $ZnS_6(N\text{-MeIm})_6$ (0.425 g, 1.0×10^{-3} mol, orange crystals) was dissolved in OAm (50 cm^3) to give an orange solution. The solution was heated to 300 °C and held at this temperature for 30 min, then allowed to cool. A slight darkening in color was observed at 140 °C, but the solution became light yellow by 300 °C. Upon cooling a cloudy white suspension formed. The reaction mixture was centrifuged to produce a white precipitate and a clear yellow supernatant. The supernatant was discarded and the precipitate was resuspended in toluene (20 cm^3) to give a clear, colorless solution. Upon addition of acetone (25 cm^3) a cloudy white suspension formed. Centrifugation produced a white precipitate and a clear colorless supernatant. The supernatant was discarded and this procedure was repeated twice. The precipitate was dried in vacuo overnight, and ground into a fine, off-white powder.

Characterization. TEM measurements were performed on a JEOL 2010 TEM operated at 200 kV. TEM samples were prepared by placing a drop of toluene suspension on a carbon-coated copper TEM grid and evaporating to dryness. XRD was performed on a Philips PW1050 diffractometer using Cu K_α radiation with a graphite secondary monochromator. UV−visible (UV−vis) and photoluminescence (PL) spectroscopy were performed on a Perkin-Elmer Cary 100 spectrophotometer and a Horiba Jobin-Yvon Fluorolog FL-1057 fluorometer, respectively. Samples were prepared as dilute suspensions in spectroscopic grade cyclohexane. Thermogravimetric analysis (TGA) of the complexes was performed on a Shimadzu TGA-50 apparatus, using approximately 10 mg of material contained in a nickel pan, and blanketed with a flow of nitrogen (50 cm^3 min^{-1}).

Hazards. Note that nickel sulfides are carcinogens.

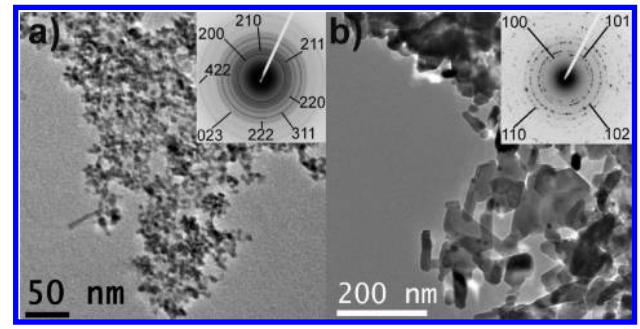

Figure 1. (a) TEM image of NiS_2 nanocrystals inset SAED pattern indexed to NiS_2. (b) TEM image of α-$Ni_{1-x}S$ nanocrystals inset SAED pattern indexed to NiAs-type α-$Ni_{1-x}S$.

Results and Discussion

Solid State Decomposition of Metal Polysulfide Complexes. TGA was used to assess the decomposition of the metal polysulfide complexes in the solid state (data not shown). Complete removal of *N*-MeIm ligands from the complexes occurred by 250 °C for $[Ni(N\text{-MeIm})_6]S_8$ and $[Fe(N\text{-MeIm})_6]S_8$, and by 290 °C for $ZnS_6(N\text{-MeIm})_2$, respectively. A reaction temperature in excess of the highest metal polysulfide complex decomposition temperature was chosen for the solution phase decomposition reactions (300 °C), in order to ensure complete decomposition of the precursor complexes and the formation of highly crystalline binary metal sulfide nanocrystals.

Nickel Sulfide Nanocrystals. Thermal decomposition of $[Ni(N\text{-MeIm})_6]S_8$ by rapid injection into oleylamine preheated to 300 °C, followed by immediate cooling, resulted in the formation of spherical NiS_2 nanocrystals (as shown in Figure 1a) with an average diameter of 6 ± 1 nm as determined from TEM measurements (see the Supporting Information for histogram of TEM size measurements). This value was in agreement with the average crystallite size of 10 ± 4 nm determined from Scherrer analysis of the XRD pattern, indicating that the NiS_2 nanocrystals are monocrystalline. SAED (Figure 1a, inset) and XRD (Figure 2, lines a and b) confirmed the sample to be pure cubic NiS_2, with no additional crystalline phases present. EDS measurements determined the composition of the sample to be Ni:S 1:2, as is appropriate for stoichiometric NiS_2.

Thermal decomposition of $[Ni(N\text{-MeIm})_6]S_8$ by gradual heating in oleylamine to 300 °C led to the formation of α-$Ni_{1-x}S$ nanocrystals with a wide size distribution and a variety of faceted morphologies, as shown in Figure 1b. The average crystallite size was determined to be 45 ± 15 nm by Scherrer analysis. SAED (Figure 1b inset) and XRD (Figure 2, lines c and d) confirmed the sample to be NiAs-type α-$Ni_{1-x}S$, with no additional crystalline phases present. The composition was determined to be Ni:S 1:1 by EDS measurements, indicating

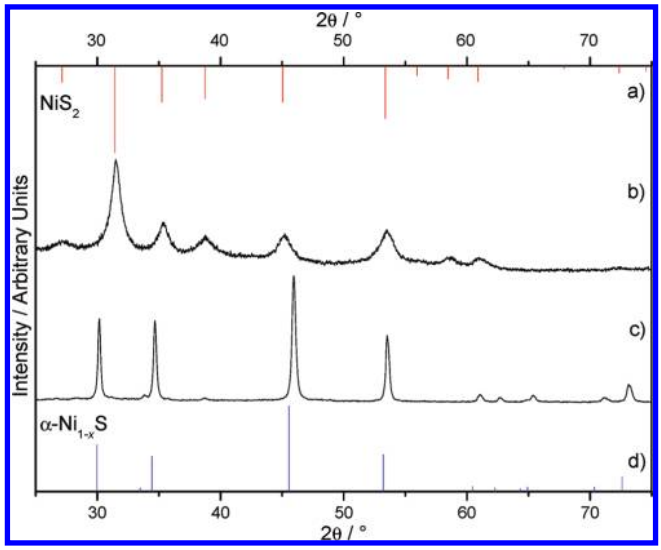

Figure 2. XRD patterns of (a) reference for NiS_2, (b) NiS_2 nanocrystals, (c) α-$Ni_{1-x}S$ nanocrystals, and (d) reference for α-$Ni_{1-x}S$.

the phase was the stoichiometric end member of the α-$Ni_{1-x}S$ composition range. The irregular morphology of some α-$Ni_{1-x}S$ crystallites makes it difficult to judge whether they are mono- or polycrystalline.

Burst nucleation of NiS_2 nanocrystals initiated by rapid injection of $[Ni(N\text{-MeIm})_6]S_8$ led to a high degree of monodispersity, whereas when $[Ni(N\text{-MeIm})_6]S_8$ was heated slowly, α-$Ni_{1-x}S$ particles with a wide size distribution resulted, presumably due to continuous nucleation and size-defocusing growth processes. The reaction duration was found to be a critical factor in controlling phase and phase-purity as the initially nucleated NiS_2 phase was observed to rapidly convert to α-$Ni_{1-x}S$ at 300 °C, with an associated change in particle morphology from spherical nanocrystals to polydisperse, faceted crystallites. A limited reaction duration, as given by cooling immediately after injection, was required to produce pure NiS_2. Despite the limited reaction duration, the NiS_2 nanocrystal samples were highly crystalline as evidenced by SAED and XRD.

To the best of our knowledge this constitutes the first synthesis of monodisperse NiS_2 nanocrystals, as previously published syntheses of nickel sulfide nanocrystals have predominantly produced Ni_3S_4,[11] α-$Ni_{1-x}S$,[20,21] or β-NiS.[21] The longer reaction times of 1[11,21] or 6[20] h used in the aforementioned syntheses likely explain the absence of NiS_2, given the evidence of the limited thermal stability of nanocrystalline NiS_2 found in this work.

The irregularly shaped α-$Ni_{1-x}S$ nanocrystals produced by the gradual heating of $[Ni(N\text{-MeIm})_6]S_8$ to 300 °C were similar in size and morphology to those produced previously.[21] The selective formation of α-$Ni_{1-x}S$ is a consequence of the reaction temperature of 300 °C favoring the high temperature α-$Ni_{1-x}S$ phase over the low temperature Ni_3S_4 or β-NiS phases.[28]

Iron Sulfide Nanocrystals. Thermal decomposition of $[Fe(N\text{-MeIm})_6]S_8$ by rapid injection into oleylamine preheated to 300 °C, followed by rapid cooling, led to the formation of Fe_3S_4 nanocrystals with a variety of faceted morphologies as shown in Figure 3a. Scherrer analysis determined the average crystallite size to be 16 ± 1 nm, which was consistent with TEM observations. SAED (Figure 3a, inset) and XRD (Figure 4, lines a and b) confirmed the sample as the cubic spinel Fe_3S_4, with no indication of the presence of additional crystalline phases. The composition of the sample was determined to be Fe:S

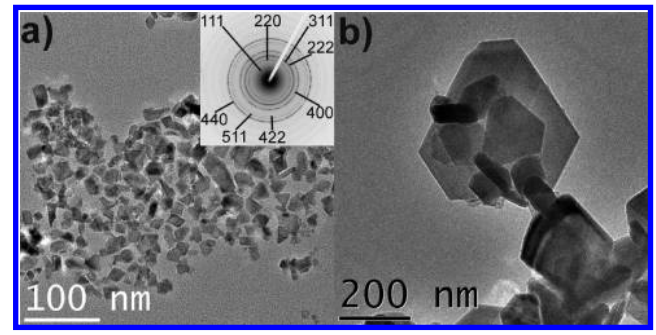

Figure 3. (a) TEM image of Fe_3S_4 nanocrystals inset SAED pattern indexed to Fe_3S_4. (b) TEM image of $Fe_{1-x}S$ nanocrystals.

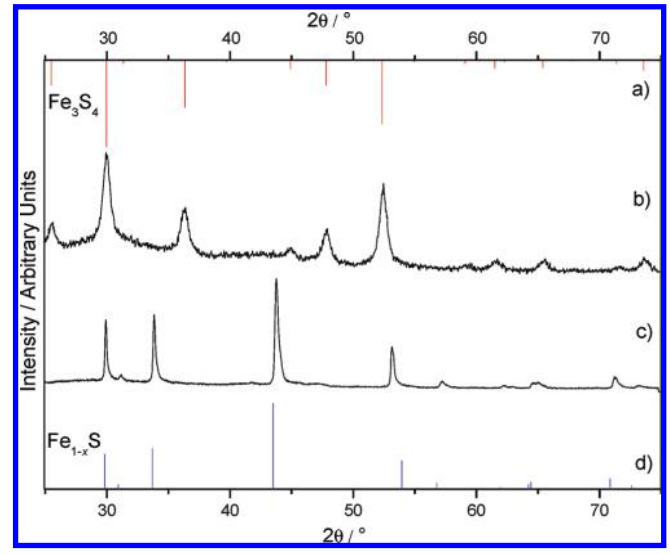

Figure 4. XRD patterns of (a) reference for Fe_3S_4, (b) Fe_3S_4 nanocrystals, (c) $Fe_{1-x}S$ nanocrystals, and (d) reference for $Fe_{1-x}S$.

47:53 by EDS measurements, which is somewhat more iron-rich than the composition of 43:57 expected for stoichiometric Fe_3S_4, however nonstoichiometry has been observed previously in Fe_3S_4 samples.[29]

Reaction of $[Fe(N\text{-MeIm})_6]S_8$ in oleylamine at 300 °C for 4 h resulted in the formation of submicrometer $Fe_{1-x}S$ crystallites with a variety of highly faceted morphologies as shown in Figure 3b. Scherrer analysis determined the average crystallite size to be 70 ± 50 nm. XRD (Figure 4, lines c and d) confirmed the sample to be hexagonal NiAs-type $Fe_{1-x}S$, with no indication of the presence of additional crystalline phases. EDS measurements determined the composition to be Fe:S 1:1, the stoichiometric limit of $Fe_{1-x}S$.

Reaction of $[Fe(N\text{-MeIm})]S_8$ at 300 °C for durations less than 4 h led to mixtures of Fe_3S_4 and $Fe_{1-x}S$, indicating that during the course of the reaction the initially nucleated Fe_3S_4 phase was converted to the thermally more stable $Fe_{1-x}S$ phase.[30,31] Fe_3S_4 itself has a narrow thermal stability range, with a decomposition temperature of approximately 190 °C, whereas nucleation of tetragonal FeS is favored at lower temperatures.[30] The preparation of pure Fe_3S_4 is, as a consequence, notoriously difficult.[32] Therefore very limited reaction times at high temperature, as given by injection of $[Fe(N\text{-MeIm})_6]S_8$ at 300 °C followed by immediate cooling, were found necessary in order to obtain pure samples of crystalline Fe_3S_4.

Similarly to the case of $[Ni(N\text{-MeIm})_6]S_8$, burst nucleation initiated by the rapid injection of $[Fe(N\text{-MeIm})_6]S_8$ led to a relatively narrow size distribution for the resulting Fe_3S_4 nanocrystals, whereas the $Fe_{1-x}S$ nanocrystals produced by

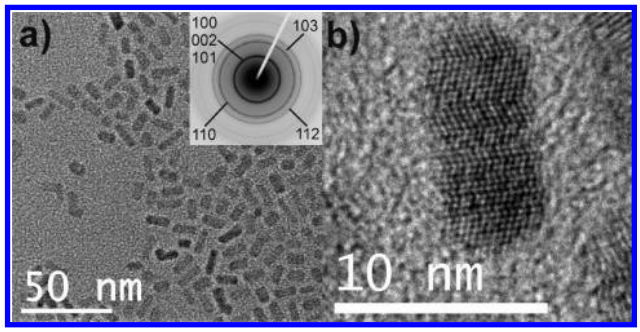

Figure 5. (a) TEM image of ZnS nanorods inset SAED pattern indexed to wurtzite ZnS. (b) High resolution TEM image of a single ZnS nanorod.

gradual heating of $[Fe(N\text{-MeIm})_6]S_8$ were observed to have a wider size distribution. The variance in the average crystallite size for $Fe_{1-x}S$ determined by Scherrer analysis (70 ± 50 nm) was however found to be partially a consequence of the highly anisotropic platy morphologies. The faceted morphologies of both the $Fe_{1-x}S$ and Fe_3S_4 nanocrystals produced from $Fe(N\text{-MeIm})_6]S_8$, and the good correspondence between Scherrer analysis and TEM observations supports the contention that the nanocrystals are in general monocrystalline.

The decomposition of $[Fe(N\text{-MeIm})_6]S_8$ to Fe_3S_4 is notable as only the second published synthesis of pure, crystalline Fe_3S_4 nanocrystals with a well-defined size distribution.[19] The synthesis of $Fe_{1-x}S$ crystals is more prevalent in the literature,[18,19] yet the high degree of crystallinity and phase-purity attained by the decomposition of $[Fe(N\text{-MeIm})_6]S_8$ to $Fe_{1-x}S$ recommends its use as a single-source precursor for this phase as well.

ZnS Nanorods. Thermal decomposition of $ZnS_6(N\text{-MeIm})_2$ at 300 °C for 30 min resulted in the formation of 11×5 nm ZnS nanorods as shown in Figure 5a. A high degree of monodispersity was observed in both the lengths and widths of the nanorods (see the Supporting Information for histograms of TEM size measurements). A high resolution micrograph of a single nanorod shown in Figure 5b demonstrates the single-crystalline nature of the rods. The SAED pattern of an ensemble of nanorods shown as an inset in Figure 5a was indexed to the hexagonal wurtzite polymorph of ZnS. An XRD pattern of the ZnS nanorods (Figure 6) was determined by Rietveld refinement to be predominantly of the wurtzite polymorph, with a small contribution from the cubic zinc blende polymorph (see the Supporting Information for details). EDS measurements determined the composition of the sample to be Zn:S 1:1, as is appropriate for stoichiometric ZnS.

$ZnS_6(N\text{-MeIm})_2$ was decomposed by rapid injection into oleylamine preheated to 300 °C, and aliquots of the reaction mixture were removed in order to monitor the progress of the reaction. It was found that ZnS nanorods had formed already in the aliquot removed immediately after injection. The optimum reaction duration, in terms of the monodispersity and crystallinity of the ZnS nanorods, was found to be 30 min.

UV−vis and PL spectra of a sample of ZnS nanorods are shown in Figure 7. The UV−vis spectrum features a sharp absorption onset at 340 nm and an excitonic absorption band centered at 320 nm, which is slightly blue-shifted from the band gap of bulk ZnS (330 nm).[8] The PL spectrum for the ZnS nanorods (excited at 280 nm) featured a sharp emission maximum at 325 nm and a broad emission peak centered around 400 nm. A PLE (Photoluminescence Excitation) spectrum (see the Supporting Information) for an emission wavelength of 330 nm showed an excitation maximum at 310 nm, which falls

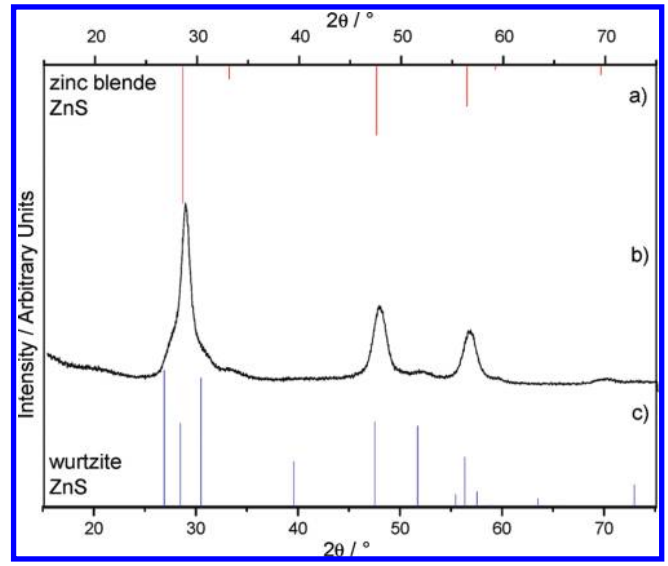

Figure 6. XRD patterns of (a) reference of zinc blende ZnS, (b) ZnS nanorods, and (c) reference of wurtzite ZnS.

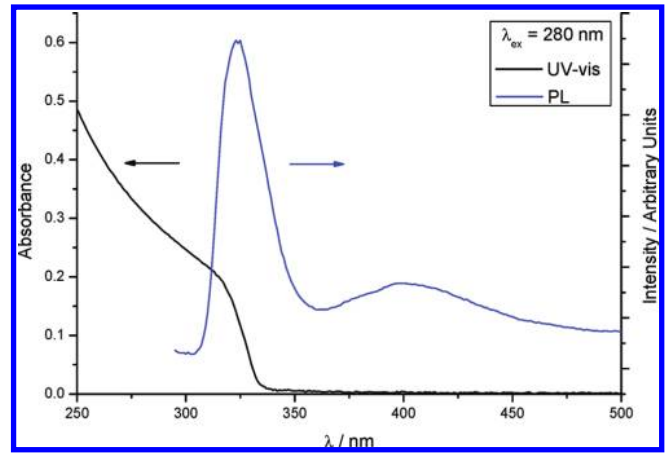

Figure 7. UV−vis absorption and PL spectra of ZnS nanorods.

within the main UV−vis excitonic absorption band, whereas the PLE spectrum for an emission wavelength of 410 nm displayed a broad excitation band above 325 nm. Hence, the sharp emission peak at 325 nm was assigned to band edge luminescence, while the lower energy peak at 400 nm was assigned to trap state emission. These optical features and assignments are in good agreement with previous studies on ZnS nanocrystals and nanorods.[33,34] Given that trap state emission can be the dominant optical feature of ZnS containing sulfur vacancies,[34] the relatively low ratio of trap state to band edge emission observed for samples in this paper can be taken as an indication of the high quality of the ZnS nanorods synthesized from $ZnS_6(N\text{-MeIm})_2$.

The degree of monodispersity of the ZnS nanorods produced from $ZnS_6(N\text{-MeIm})_2$, in both length ($\sigma = 22\%$) and width ($\sigma = 17\%$), is similar to that of previous studies.[34,35] However this combined with the simplicity of using a single-source precursor for synthesis, the high degree of crystallinity obtained despite the relatively mild reaction conditions used, and the strength of band edge versus trap state emission, recommend $ZnS_6(N\text{-MeIm})_2$ as a single-source precursor for ZnS nanorods.

Metal Polysulfide Complexes As Single-Source Precursors. With metal to sulfur ratios of 1:6 to 1:8, the metal polysulfide complexes described in this paper contain a significant excess of sulfur with respect to binary metal sulfides (which typically

have metal to sulfur ratios of between 3:2 and 1:2). As demonstrated above, this allows the synthesis of phases with a range of compositions by altering reaction conditions such as reaction temperature and duration, without requiring any alteration in the precursor itself, or alteration in the ratio of two independent precursors. The excess of sulfur present in the precursors was not detrimental to the synthesis, given the use of a solvent such as oleylamine, in which elemental sulfur has appreciable solubility. Excess sulfur was observed to remain dissolved even after the reaction mixture was cooled to room temperature, and could be separated from the desired product simply by washing with a nonpolar solvent, such as toluene. With the exception of the excess sulfur mentioned above, metal polysulfide complexes possess the advantage of producing no nonvolatile byproducts, such as halide ions, which can be difficult to separate, and may adversely affect the quality of products.[34,36,37] In fact, the excess of sulfur in metal polysulfide complexes can be beneficial in limiting the number of sulfur vacancies in the product, as was seen in the case of ZnS nanorods, which had a relatively low level of trap state emission associated with vacancies.

Conclusions

It has been demonstrated that transition metal polysulfide complexes can be flexible and robust single-source precursors for the synthesis of high-quality metal sulfide nanocrystals, with $[M(N\text{-MeIm})_6]S_8$ (M = Fe, Ni) and $ZnS_6(N\text{-MeIm})_2$ being used to produce phase-pure samples of Fe_3S_4 and $Fe_{1-x}S$ nanocrystals, NiS_2 and α-$Ni_{1-x}S$ nanocrystals, and ZnS nanorods, respectively. These complexes are easily and cheaply prepared from elemental sulfur and the relevant metal powder by reaction in neat *N*-MeIm, and their use therefore represents an elegant two-step synthesis of binary metal sulfide nanocrystals from the elements, in a manner that allows an exceptional degree of experimental control.

Acknowledgment. The authors thank the MacDiarmid Institute for Advanced Materials and Nanotechnology for funding and Dr. Kirsten Edgar of Victoria University of Wellington for helpful discussions. RDT thanks the Foundation for Science, Research and Technology for funding through grant PROJ-13733-NMTS.

Supporting Information Available: Details of the synthesis of the metal polysulfide complexes $[M(N\text{-MeIm})_6]S_8$ (M = Fe, Ni) and $ZnS_6(N\text{-MeIm})_2$; Rietveld refinement of the XRD pattern of ZnS nanorods; PLE spectra of ZnS nanorods; and histograms of the particle size distributions of NiS_2 nanocrystals and ZnS nanorods determined from TEM measurements. This material is available free of charge via the Internet at http://pubs.acs.org.

References and Notes

(1) Gaponenko, S. V. *Optical Properties of Semiconductor Nanocrystals*; Cambridge University Press: Cambridge, 1998.
(2) Leslie-Pelecy, D. L.; Rieke, R. D. *Chem. Mater.* **1996**, *8*, 1770.
(3) Ying, J. Y. *Chem. Eng. Sci.* **2006**, *61*, 1540.
(4) Murray, C. B.; Norris, D. J.; Bawendi, M. G. *J. Am. Chem. Soc.* **1993**, *115*, 8706.
(5) Wang, D.-S.; Zheng, W.; Hao, C.-H.; Peng, Q.; Li, Y.-D. *Chem.—Eur. J.* **2009**, *15*, 1870.
(6) Zhong, X.; Liu, S.; Zhang, Z.; Li, L.; Wei, Z.; Knoll, W. *J. Mater. Chem.* **2004**, *14*, 2790.
(7) Ehlert, O.; Osvet, A.; Batentschuk, M.; Winnacker, A.; Nann, T. *J. Phys. Chem. B* **2006**, *110*, 23175.
(8) Quan, Z.; Wang, Z.; Yang, P.; Lin, J.; Fang, J. *Inorg. Chem.* **2007**, *46*, 1354.
(9) Chen, X.; Zhang, X.; Wan, J.; Wang, Z.; Qian, Y. *Chem. Phys. Lett.* **2005**, *403*, 396.
(10) Tilley, R. D.; Jefferson, D. A. *J. Phys. Chem. B* **2002**, *106*, 10895.
(11) Ghezelbash, A.; Korgel, B. A. *Langmuir* **2005**, *21*, 9451.
(12) Sigman, M. B. J.; Ghezelbash, A.; Hanrath, T.; Saunders, A. E.; Lee, F.; Korgel, B. A. *J. Am. Chem. Soc.* **2003**, *125*, 16050.
(13) Revaprasadu, N.; Mlondo, S. N. *Pure Appl. Chem.* **2006**, *78*, 1691.
(14) Vittal, J. J.; Ng, M. T. *Acc. Chem. Res.* **2006**, *39*, 869.
(15) Fan, D.; Afzaal, M.; Mallik, M. A.; Nguyen, C. Q.; Thomas, P. J.; O'Brien, P. *Coord. Chem. Rev.* **2007**, *251*, 1878.
(16) Malik, M. A.; Revaprasadu, N.; O'Brien, P. *Chem. Mater.* **2001**, *13*, 913.
(17) Barrelet, C. J.; Wu, Y.; Bell, D. C.; Lieber, C. M. *J. Am. Chem. Soc.* **2003**, *125*, 11498.
(18) Han, W.; Gao, M. *Cryst. Growth Des.* **2008**, *8*, 1023.
(19) Vanitha, P. V.; O'Brien, P. *J. Am. Chem. Soc.* **2008**, *130*, 17256.
(20) Geng, B.; Liu, X.; Ma, J.; Du, Q. *Mater. Sci. Eng., B* **2007**, *145*, 17.
(21) Tian, L.; Yep, L. Y.; Ong, T. T.; Yi, J.; Ding, J.; Vittal, J. J. *Cryst. Growth Des.* **2009**, *9*, 353.
(22) Ramli, E.; Rauchfuss, T. B.; Stern, C. L. *J. Am. Chem. Soc.* **1990**, *112*, 4043.
(23) Dev, S.; Rauchfuss, T. B.; Ramli, E.; Stern, C. L. *J. Am. Chem. Soc.* **1990**, *112*, 6385.
(24) Dev, S.; Ramli, E.; Rauchfuss, T. B.; Wilson, S. R. *Inorg. Chem.* **1991**, *30*, 2514.
(25) Paul, P. P.; Rauchfuss, T. B.; Wilson, S. R. *J. Am. Chem. Soc.* **1993**, *115*, 3316.
(26) Verma, A. K.; Rauchfuss, T.; Wilson, S. R. *Inorg. Chem.* **1995**, *34*, 3072.
(27) Rauchfuss, T. B. *Inorg. Chem.* **2004**, *43*, 14.
(28) Kullerud, G.; Yund, R. A. *J. Petrol.* **1962**, *3*, 126.
(29) Spender, M. R.; Coey, J. M. D.; Morrish, A. H. *Can. J. Phys.* **1972**, *50*, 2313.
(30) Uda, M. *Z. Anorg. Allg. Chem.* **1967**, *350*, 105.
(31) Wang, H.; Salveson, I. *Phase Transitions* **2005**, *78*, 547.
(32) Uda, M. *Am. Mineral.* **1965**, *50*, 1487.
(33) Wageh, S.; Ling, Z. S.; Xu-Rong, X. *J. Cryst. Growth* **2003**, *255*, 332.
(34) Yu, H. J.; Joo, J.; Park, H. M.; Baik, S. I.; Kim, Y. W.; Kim, S. C.; Hyeon, T. *J. Am. Chem. Soc.* **2005**, *127*, 5662.
(35) Thomas, P. J.; Christian, P.; Daniels, S.; Li, Y.; Wang, Y. S.; O'Brien, P. *Pure Appl. Chem.* **2006**, *78*, 1651.
(36) Qu, L.; Peng, Z. A.; Peng, X. *Nano Lett.* **2001**, *1*, 333.
(37) Xu, Y.; Al-Salim, N.; Bumby, C. W.; Tilley, R. D. *J. Am. Chem. Soc.* **2009**, *131*, 15990.

JP910354Q